Structural Engineering and Mechanics, Vol. 44, No. 5 (2012) 585-600
DOI: http://dx.doi.org/10.12989/sem.2012.44.5.585

Modified Tikhonov regularization in model updating for damage identification

J. Wang* and Q.S. Yang[a]

School of Civil Engineering, Beijing Jiaotong University, Beijing, P.R. China

(Received August 22, 2011, Revised September 24, 2012, Accepted October 24, 2012)

Abstract. This paper presents a Modified Tikhonov Regularization (MTR) method in model updating for damage identification with model errors and measurement noise influences consideration. The identification equation based on sensitivity approach from the dynamic responses is ill-conditioned and is usually solved with regularization method. When the structural system contains model errors and measurement noise, the identified results from Tikhonov Regularization (TR) method often diverge after several iterations. In the MTR method, new side conditions with limits on the identification of physical parameters allow for the presence of model errors and ensure the physical meanings of the identified parameters. Chebyshev polynomial is applied to approximate the acceleration response for moderation of measurement noise. The identified physical parameter can converge to a relative correct direction. A three-dimensional unsymmetrical frame structure with different scenarios is studied to illustrate the proposed method. Results revealed show that the proposed method has superior performance than TR Method when there are both model errors and measurement noise in the structure system.

Keywords: damage identification; noise; model error; modified Tikhonov regularization; model updating; sensitivity; iteration

1. Introduction

Most structures are subject to damage during their service lives due to unfavorable factors such as environmental loads, fatigue effects, corrosion effects, material aging and etc. Early damage detection and structural condition assessment are necessary for a structure such that timely maintenance and repair of structural damage can be properly scheduled. This is vital to ensure the overall safety in the service life of a structure. Structural damage may, in general, lead to changes in the properties of a structure (mass, stiffness and damping) and these changes will in turn affect its dynamic responses and characteristics. This fact forms the basis of vibration-based damage identification techniques.

There are many vibration-based damage detection methods. The identification approaches are mainly based on the changes in natural frequencies (Cawley and Adams 1979, Hassiotis and Jeong 1993, Bicanic and Chen 1997), mode shape curvature (Pandey *et al.* 1991), modal flexibility (Toksoy and Aktan 1994) and modal strain energy (Osegueda *et al.* 1997) which are usually taken

*Corresponding author, Ph.D. Student, E-mail: 05121303@bjtu.edu.cn
[a]Professor, E-mail: qshyang@bjtu.edu.cn

as the measured information to identify local damage in the frequency domain.

Comparing to the frequency domain approach, the time domain approach takes advantage of the time dimension with plenty of measured data to formulate an over-determined set of equations for the finite element model updating and damage detection. Lu and Law (2007) proposed a sensitivity-based approach for identifying the local damages in a structure directly from the measured dynamic responses. Sensitivity matrix of the response was calculated and directly used to locate and quantify the damage severity.

This paper does not introduce another method for damage identification. A Modified Tiknonov Regularization (MTR) Method is proposed with the dynamic response sensitivity approach. Damage in a structure can be defined in terms of a stiffness reduction factor. The change in the global stiffness matrix is $\Delta\mathbf{K} = \sum_{i=1}^{ne} \alpha_i \mathbf{K}_i$, in which $\mathbf{K}_i$ is the stiffness matrix of the ith element, ne is the number of elements in the structure, α_i is the stiffness reduction factor of the ith element. The stiffness matrix of the damaged structure then becomes $\mathbf{K} + \Delta\mathbf{K}$. The notations on the stiffness change in the following study are defined as follows: α and $\Delta\alpha$ are the total stiffness change and the increment of an iteration with the size of $ne \times 1$, respectively. The superscript k in α^k and $\Delta\alpha^k$ denotes results obtained for the kth iteration. α_i and $\Delta\alpha_i$ are the ith element of the vector α and $\Delta\alpha$.

The inverse problem based on sensitivity approach is often associated with the solution of a set of equations of $\mathbf{A}\mathbf{x} - \mathbf{b} = 0$. Like many other inverse problems, this kind of equations is ill-conditioned and the classical least-squares solution from the minimization of the norm $\|\mathbf{A}\mathbf{x} - \mathbf{b}\|_2^2$ would be inaccurate when there are model errors and measurement noise in practice. This kind of problem is usually solved by regularization method (Tikhonov 1963, Hansen 1987, Hansen 1992, Vogel 2002). From experiences gained in model updating with simulated structures, Tikhonov Regularization (TR) method is found to give the optimal solution when there is no noise or very small noise in the measurement. The solution norm $\|\mathbf{x}_\lambda\|_2^2$ is added to the residual norm $\|\mathbf{A}\mathbf{x}_\lambda - \mathbf{b}\|_2^2$ as a side condition, and the regularized solution can be obtained from the minimization of $\|\mathbf{A}\mathbf{x}_\lambda - \mathbf{b}\|_2^2 + \lambda^2 \|\mathbf{x}_\lambda\|_2^2$. Parameter λ is the regularization parameter controlling the weight of the solution norm and the residual norm, and it can usually be determined by the L-curve method (Hansen 1992). However, some of the solutions obtained from the TR method exceed their physical limits ($-1 \le \alpha_i \le 0$) and lose their physical meanings. Li and Law (2010) proposed an Adaptive Tikhonov Regularization Method for damage detection based on nonlinear model updating. The discrimination of possible damaged elements and undamaged elements is performed from results obtained in previous iterations via a new side condition which aims at (a) to limit the local change in damaged structural elements in each iteration; and (b) to ensure the variation of other undamaged elements close to zero. This method was proved effective even with noise contamination in the measurements. However, this new side condition does not take care of all possible variations of the stiffness change, and in particular, the effect of initial model errors.

In the proposed MTR method, new side conditions with limits on the identification of physical parameters allow for the presence of model errors and ensure the physical meanings of the identified parameters. Chebyshev polynomial (Ni and Chen 2009) is applied to approximate the acceleration response for moderation of measurement noise. The identified physical parameter can converge to a relative correct direction. A three-dimensional unsymmetrical frame structure with different scenarios is studied to illustrate the proposed method. Results from simulations show that the proposed method has superior performance than the TR method when there are both model errors and measurement noise.

2. Forward problem

2.1 Dynamic response of a structure

For a general finite element model of a time-invariant N degrees-of-freedom (DOFs) damped structure, the equation of motion can be written as

$$\mathbf{M}\ddot{\mathbf{x}} + \mathbf{C}\dot{\mathbf{x}} + \mathbf{K}\mathbf{x} = \mathbf{L}\mathbf{F} \tag{1}$$

where $\mathbf{M}$, $\mathbf{C}$, and $\mathbf{K}$ are the mass, damping and stiffness matrices of the structural system respectively. Rayleigh damping is adopted which is of the form

$$\mathbf{C} = a_1 \cdot \mathbf{M} + a_2 \cdot \mathbf{K} \tag{2}$$

where a_1 and a_2 are constants to be determined from the modal damping ratios of two modes. $\ddot{\mathbf{x}}$, $\dot{\mathbf{x}}$ and $\mathbf{x}$ are vectors of acceleration, velocity and displacement of the structural system respectively. $\mathbf{F}$ is the vector of external excitation forces with matrix $\mathbf{L}$ mapping these forces to the associated DOFs of the structure. If the external excitation and the finite element model of the structure are known, responses $\ddot{\mathbf{x}}$, $\dot{\mathbf{x}}$ and $\mathbf{x}$ in Eq. (1) can be solved using the step-by-step Newmark-β integration method.

2.2 Sensitivity of response in time domain

Differentiate Eq. (1) with respect to α_i, we have

$$\mathbf{M}\frac{\partial \ddot{\mathbf{x}}}{\partial \alpha_i} + \mathbf{C}\frac{\partial \dot{\mathbf{x}}}{\partial \alpha_i} + \mathbf{K}\frac{\partial \mathbf{x}}{\partial \alpha_i} = -\frac{\partial \mathbf{K}}{\partial \alpha_i}\mathbf{x} - a_2\frac{\partial \mathbf{K}}{\partial \alpha_i}\dot{\mathbf{x}} \tag{3}$$

where $\partial\ddot{\mathbf{x}}/\partial\alpha_i$, $\partial\dot{\mathbf{x}}/\partial\alpha_i$, $\partial\mathbf{x}/\partial\alpha_i$ are vectors of the acceleration, velocity and displacement sensitivities with respect to the stiffness fractional change respectively. Since $\mathbf{x}$ and $\dot{\mathbf{x}}$ have been obtained from Eq. (1), the right-hand side of Eq. (3) can be considered as an equivalent forcing function, and Eq. (3) is of the same form as Eq. (1). The sensitivities $\partial\ddot{\mathbf{x}}/\partial\alpha_i$, $\partial\dot{\mathbf{x}}/\partial\alpha_i$ and $\partial\mathbf{x}/\partial\alpha_i$ can be also obtained by step-by-step Newmark-β integration method.

3. Inverse problem

In the forward analysis, the dynamic responses and their sensitivities with respect to the structural parameters of a finite element system can be obtained from Eq. (1) and Eq. (3). In the inverse problem, the stiffness fractional change will be identified from the measured responses at the accessible DOFs. The most commonly used measured response is acceleration because of its ease of measurement.

An error function, defined as the difference between the calculated responses from the updated finite element model and the measured acceleration responses of the structure, can be written as

$$\Delta\ddot{\mathbf{x}} = \ddot{\mathbf{x}}_m - \ddot{\mathbf{x}}_{cal} \tag{4}$$

The identification equation can be expressed as the first order Taylor expansion of the acceleration responses (Lu and Law 2007)

$$\mathbf{S} \cdot \alpha = \Delta \ddot{\mathbf{x}} \tag{5}$$

where $\mathbf{S}$ is the acceleration response sensitivity matrix that can be calculated from Eq. (3), and it can be written as (Lu and Law 2007)

$$\mathbf{S} = \begin{bmatrix} \mathbf{S}_1 \\ \mathbf{S}_2 \\ \cdots \\ \mathbf{S}_i \\ \cdots \\ \mathbf{S}_{nt} \end{bmatrix} \text{ with } \mathbf{S}_i = \begin{bmatrix} \frac{\partial \ddot{\mathbf{x}}_1(t_i)}{\partial \alpha_1} & \frac{\partial \ddot{\mathbf{x}}_1(t_i)}{\partial \alpha_2} & \frac{\partial \ddot{\mathbf{x}}_1(t_i)}{\partial \alpha_3} & \cdots & \frac{\partial \ddot{\mathbf{x}}_1(t_i)}{\partial \alpha_{ne}} \\ \frac{\partial \ddot{\mathbf{x}}_2(t_i)}{\partial \alpha_1} & \frac{\partial \ddot{\mathbf{x}}_2(t_i)}{\partial \alpha_2} & \frac{\partial \ddot{\mathbf{x}}_2(t_i)}{\partial \alpha_3} & \cdots & \frac{\partial \ddot{\mathbf{x}}_2(t_i)}{\partial \alpha_{ne}} \\ \frac{\partial \ddot{\mathbf{x}}_3(t_i)}{\partial \alpha_1} & \frac{\partial \ddot{\mathbf{x}}_3(t_i)}{\partial \alpha_2} & \frac{\partial \ddot{\mathbf{x}}_3(t_i)}{\partial \alpha_3} & \cdots & \frac{\partial \ddot{\mathbf{x}}_3(t_i)}{\partial \alpha_{ne}} \\ \vdots & \vdots & \vdots & \vdots & \vdots \\ \frac{\partial \ddot{\mathbf{x}}_{Nsensor}(t_i)}{\partial \alpha_1} & \frac{\partial \ddot{\mathbf{x}}_{Nsensor}(t_i)}{\partial \alpha_2} & \frac{\partial \ddot{\mathbf{x}}_{Nsensor}(t_i)}{\partial \alpha_3} & \cdots & \frac{\partial \ddot{\mathbf{x}}_{Nsensor}(t_i)}{\partial \alpha_{ne}} \end{bmatrix} \tag{6}$$

where nt is the total number of time sampling points, N_{sensor} is the number of sensors. $\mathbf{S}$ is a two dimensional matrix representing three-dimensional array, with one dimension of time, one dimension of measured DOFs and the other dimension of the number of structural parameters to be identified.

The model updating technique is required. An analytical model of the target structure is treated as the reference model, and the measurements from the damaged structure will be used to update the reference model with iterations. The vector of structural physical parameters can be identified through model updating. The damage identification equation for the (k+1)th iteration can be written as

$$\mathbf{S}^k \Delta \alpha^{k+1} = \Delta \ddot{\mathbf{x}}^k \tag{7}$$

where $\mathbf{S}^k$ and $\Delta \ddot{\mathbf{x}}^k$ are obtained from the kth iteration.

Convergence is considered achieved when the following criterion is met

$$\frac{\left\| \alpha^{k+1} - \alpha^k \right\|}{\left\| \alpha^{k+1} \right\|} \leq Tolerance \tag{8}$$

where α^k is the stiffness fractional change from the kth iterative step. *Tolerance* is a small value to be defined.

The final fractional change in the stiffness of the ith element after nth iteration is

$$\alpha_i = \alpha_i^0 + \Delta \alpha_i^1 + \Delta \alpha_i^2 + \ldots + \Delta \alpha_i^n \tag{9}$$

in which n is the number of iterations, α_i^0 is the assumed initial stiffness reduction factor that is usually assumed equal to 0.0.

The relative percentage error in the identified result is defined as

$$Relative\ error = \frac{\left\| \alpha_{id} - \alpha_{real} \right\|}{\left\| \alpha_{real} \right\|} \times 100\% \tag{10}$$

where α_{id} is the vector of identified stiffness reduction factors and α_{real} denotes the vector of real set of stiffness reduction factors.

4. MTR method

4.1 MTR method

Like many other inverse problems, Eq. (7) is ill-conditioned. This means that small perturbations can lead to unrealistically large perturbations in the update parameters, and regularization method should be taken to solve the problem. The two most common regularization methods are TR method and the truncated singular value decomposition (Golub and Van Loan 1996).

In the TR method, Eq. (7) can be solved as the minimization of the following objective function

$$J(\Delta\alpha^{k+1}) = \left\|\mathbf{S}^k\Delta\alpha^{k+1} - \Delta\ddot{\mathbf{x}}^k\right\|_2^2 + \lambda^2\left\|\Delta\alpha^{k+1}\right\|_2^2 \tag{11}$$

This function has two parts: the first part is the least-squares solution of Eq. (7); the second part limits the size of the update solutions. The regularization parameter λ controls the weight given to the solution norm $\left\|\Delta\alpha^{k+1}\right\|_2^2$ relative to the residual norm $\left\|\mathbf{S}^k\Delta\alpha^{k+1} - \Delta\ddot{\mathbf{x}}^k\right\|_2^2$.

The TR method in Eq. (11) adds a regularization term to the least-squares minimization form in order to solve the ill-conditioned problem. However, when a structural system contains model errors and measurement noise, some of the solutions obtained will exceed their limits and lose their physical meanings. The reason for this is that the TR method does have a side condition on the least-squares solution, but the range of the regularized solution is from $-\infty$ to ∞ which means the physical meaning of the solution is not ensure. In order to avoid the shortcoming of the TR method, the minimization function in the MTR method can be defined similar to the consistent regularization form (Weber *et al.* 2009, Li and Law 2010)

$$J(\Delta\alpha^{k+1}, \lambda) = \left\|\mathbf{S}^k \cdot \Delta\alpha^{k+1} - \Delta\ddot{\mathbf{x}}^k\right\|_2^2 + \lambda^2\left\|\alpha^{k+1} - \alpha^{k,*}\right\|_2^2 \tag{12}$$

When there is no model error in the finite element model of the structure, the accumulated change only exists in damaged elements with a decrease in stiffness. The range of the summation of increments of the stiffness fractional change is as follows

$$-1 \le \alpha^{k+1} \le 0 \tag{13}$$

when $k = 0$, $\alpha^{0,*} = 0$;
when $k \ge 1$

$$\alpha^{k,*} = \begin{cases} 0 & \text{if} \quad ((\alpha^k)_i > 0) \\ (\alpha^k)_i & \text{if} \quad (-1 \le (\alpha^k)_i \le 0) \\ -1 & \text{if} \quad ((\alpha^k)_i < -1) \end{cases} \tag{14}$$

However, in practice, the structure may contain initial model errors. Model errors in structure usually refer to parametric perturbations, wrong geometric properties, incorrect boundary conditions and etc. This paper only focuses on the parameter errors. With the consideration of model errors, the accumulated change (difference) not only exists in damaged elements but in all of the structure elements. Thus, a range of the stiffness fractional change is provided in the MTR method as

$$l_{low} \le \alpha^{k+1} \le l_{up} \tag{15}$$

in which l_{low} and l_{up} are the lower and upper limits. The usual limits of $-1 \le \alpha^{k+1} \le 1$ define the

general range of the stiffness change factor to ensure the physical meanings of the structure element. However, $[l_{low}, l_{up}]$ can be a narrow range with $-1 \le l_{low} \le 0$ and $0 \le l_{up} \le 1$, and it can be determined from engineering considerations like results of non-destructive tests for structural parameters. Eq. (14) can then be expressed in the MTR method as

$$\alpha^{k,*} = \begin{cases} l_{up} & \text{if} \quad ((\alpha^k)_i > l_{up}) \\ (\alpha^k)_i & \text{if} \quad (l_{low} \le (\alpha^k)_i \le l_{up}) \\ l_{low} & \text{if} \quad ((\alpha^k)_i < l_{low}) \end{cases} \tag{16}$$

To minimize the objective function in Eq. (12), the sensitivity matrix is singular value decomposed as

$$\mathbf{S}^k = \mathbf{U}\Sigma\mathbf{V}^T \tag{17}$$

where $\mathbf{U}$ and $\mathbf{V}$ are of dimensions $(N_{sensor} \times nt) \times ne$ and $ne \times ne$ respectively with $(N_{sensor} \times nt) > ne$. The vectors in $\mathbf{U}$ and $\mathbf{V}$ are orthogonal, i.e., $\mathbf{U}^T\mathbf{U} = \mathbf{V}^T\mathbf{V} = \mathbf{V}\mathbf{V}^T = \mathbf{I}_{ne \times ne}$. However, $\mathbf{U}\mathbf{U}^T \ne \mathbf{I}$, because matrix $\mathbf{U}$ contains only ne columns in the thin version of the singular value decomposition. This thin version decomposition is more economical and is usually sufficient for calculation (Weber *et al.* 2009). $\Sigma = diag(\sigma_1, \sigma_2, \ldots, \sigma_{ne})$ has the singular values σ_i arranged in a non-increasing order such that $\sigma_1 \ge \sigma_2 \ge \ldots \ge \sigma_{ne} \ge 0$.

The solution to Eq. (7) can then be obtained as a function of the regularization parameter λ

$$\begin{aligned} \Delta\alpha^{k+1} &= (\mathbf{S}_k^T\mathbf{S}_k + \lambda^2\mathbf{I})^{-1}[\mathbf{S}_k^T\Delta\ddot{\mathbf{x}}^k - \lambda^2(\alpha^k - \alpha^{k,*})] \\ &= \sum_{i=1}^{ne}(\mathbf{V}_i f_i \mathbf{x}_w - V_i(1-f_i)\mathbf{x}_v) \end{aligned} \tag{18}$$

where $\mathbf{x}_w = \mathbf{U}_i^T\Delta\ddot{\mathbf{x}}^k/\sigma_i$, $x_v = \mathbf{V}^T(\alpha^k - \alpha^{k,*})$ and f is the vector of filter factors with the expression as $f_i = \sigma_i^2/(\sigma_i^2 + \lambda^2)$, $(i = 1, 2, \ldots, ne)$. Since the range of the regularization parameter is $\sigma_1 \ge \lambda \ge \sigma_{ne}$. It is noted that regularization method makes use of the filter factors to damp the effects associated with small singular values.

4.2 Determination of regularization parameter

The L-curve method (Hansen 1992) is used for determining λ in this work. L-curve is a plot on all valid regularization parameters with the norm of the regularized solution versus the corresponding residual. The range of the regularization parameter $[\sigma_{ne}, \sigma_1]$ is divided into 2000 points for choosing the optimal λ.

The residual norm and solution norm are

$$\rho^2 = \left\|\mathbf{S}^k \cdot \Delta\alpha^{k+1} - \Delta\ddot{\mathbf{x}}^k\right\|_2^2 = \left\|\sum_{i=1}^{ne}(\mathbf{U}_i\sigma_i(f_i\mathbf{x}_w - (1-f_i)\mathbf{x}_v) - \Delta\ddot{\mathbf{x}}^k)\right\|_2^2 \tag{19}$$

$$\eta^2 = \left\|\alpha^{k+1} - \alpha^{k,*}\right\|_2^2 = \left\|\sum_{i=1}^{ne}(\mathbf{V}_i f_i \mathbf{x}_w - \mathbf{V}_i(1-f_i)\mathbf{x}_v + \alpha^k - \alpha^{k,*})\right\|_2^2 \tag{20}$$

Fig. 1 shows the generic form of the L-curve. It displays the compromise between minimization

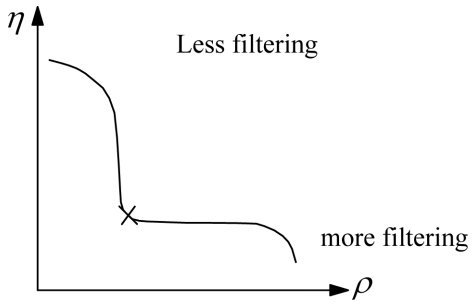

Fig. 1 Generic form of the L-curve

of these two quantities. The value of λ can be located corresponding to the maximum value of the curvature.

4.3 Moderation of the measurement noise effect

White noise is added to the calculated responses to simulate the polluted measured responses

$$\ddot{\mathbf{x}}_m = \ddot{\mathbf{x}} + E_P N_{noise} \sigma(\ddot{\mathbf{x}}) \tag{21}$$

where E_p is the percentage noise level, N_{noise} is a standard normal distribution vector with zero mean and unit standard deviation, $\sigma(\ddot{\mathbf{x}})$ is the standard deviation of the calculated acceleration response.

Since the dynamic response sensitivity approach is in time domain, Chebyshev Polynomial (Ni and Chen 2009) is applied to approximate the time history ($t \in [0, t^*]$) of the "measured" accelerations so as to moderate the influence of noise.

Firstly, the time variable $t \in [0, t^*]$ is normalized as $\tau \in [-1, 1]$ as follows

$$\tau = \frac{2}{t^*} \cdot t - 1, \quad t \in [0, t^*] \tag{22}$$

The "measured" acceleration is defined as

$$\ddot{\mathbf{x}}_{\mathbf{m}}(t) = \{\ddot{\mathbf{x}}_{\mathbf{m}1}(t) \;\; \ddot{\mathbf{x}}_{\mathbf{m}2}(t) \;\; \ldots \;\; \ddot{\mathbf{x}}_{\mathbf{m}l}(t) \;\; \ldots \;\; \ddot{\mathbf{x}}_{\mathbf{m}Nsensor}(t)\}^T \tag{23}$$

while the "measured" acceleration after curve-fitting is defined as

$$\ddot{\mathbf{x}}_{\mathbf{c}}(t) = \{\ddot{\mathbf{x}}_{\mathbf{c}1}(t) \;\; \ddot{\mathbf{x}}_{\mathbf{c}2}(t) \;\; \ldots \;\; \ddot{\mathbf{x}}_{\mathbf{c}l}(t) \;\; \ldots \;\; \ddot{\mathbf{x}}_{\mathbf{c}Nsensor}(t)\}^T \tag{24}$$

with

$$\ddot{\mathbf{x}}_{\mathbf{c}l}(t) = \sum_{i=0}^{Nm} q_i T_i(\tau), \quad \tau \in [-1, 1] \tag{25}$$

where, N_m denotes the number of terms of the Chebyshev Polynomial. The Chebyshev Polynomial T_i is determined from the following recurrence formulae

$$
\begin{aligned}
T_0(\tau) &= 1 \\
T_1(\tau) &= \tau \\
&\vdots \\
T_p(\tau) &= 2\tau T_{p-1}(\tau) - T_{p-2}(\tau)\ ; \qquad |\tau| \le 1,\ \ p \ge 2
\end{aligned} \tag{26}
$$

The coefficient of the Chebyshev Polynomial q_i can be taken as unknowns in the curve fitting via the least-squares method. The cost function which is the difference between the responses after curve-fitting and the measured responses can be written as

$$
\begin{aligned}
J_l(q_i) &= \ddot{\mathbf{x}}_{\mathbf{c}l}(t) - \ddot{\mathbf{x}}_{\mathbf{m}l}(t) \\
&= \begin{bmatrix}
T_0(\tau_1) & T_1(\tau_1) & T_2(\tau_1) & \dots & T_{N_m}(\tau_1) \\
T_0(\tau_2) & T_1(\tau_2) & T_2(\tau_2) & \dots & T_{N_m}(\tau_2) \\
T_0(\tau_3) & T_1(\tau_3) & T_2(\tau_3) & \dots & T_{N_m}(\tau_3) \\
\vdots & \vdots & \vdots & & \vdots \\
T_0(\tau_n) & T_1(\tau_n) & T_2(\tau_n) & \dots & T_{N_m}(\tau_n)
\end{bmatrix} \cdot \begin{Bmatrix} q_1 \\ q_2 \\ \vdots \\ q_{N_m} \end{Bmatrix} - \begin{Bmatrix} \mathbf{x}_{\mathbf{m}l}(t_1) \\ \mathbf{x}_{\mathbf{m}l}(t_2) \\ \vdots \\ \mathbf{x}_{\mathbf{m}l}(t_n) \end{Bmatrix},\ \tau \in [-1,1]
\end{aligned} \tag{27}
$$

in which τ is calculated by Eq. (22). q_i is obtained by minimizing the cost function in Eq. (27).

4.4 Implementation procedure

The implementation procedure in model updating via MTR method is shown as follows:

Step 1: Conduct acceleration measurements $\ddot{\mathbf{x}}_m$ at the accessible DOFs of the structure.

Step 2: The Chebyshev Polynomial is applied to approximate the "measured" responses. The vector of coefficients of Chebyshev Polynomials q_i is calculated by minimizing the cost function in Eq. (27), and the "measured" acceleration after curve-fitting can be obtained from Eq. (25).

Step 3: The range of the stiffness fractional change [l_{low}, l_{up}] is determined from engineering considerations like results of non-destructive tests.

Step 4: With the given force vector acting on the structure and the structural mass, damping and stiffness matrices of the analytical reference model updated from the last k iterations, the acceleration vector $\ddot{\mathbf{x}}_{cal}$ is obtained from Eq. (1) at the (k+1)th iterative step using Newmark-β integration method. Subsequently, the error vector $\Delta\ddot{\mathbf{x}}$ of the differences between the calculated acceleration $\ddot{\mathbf{x}}_{cal}$ and measured acceleration $\ddot{\mathbf{x}}_m$ is computed from Eq. (4).

Step 5: The sensitivity matrix $\mathbf{S}$ of the acceleration with respect to the different physical parameter of the structure is obtained from Eq. (3) using again Newmark-β integration method at (k+1)th iteration with the physical parameter vector and acceleration response vector obtained from the last k iterations.

Step 6: The sensitivity matrix $\mathbf{S}$ obtained in step 5 is singular value decomposed from Eq. (17). The side condition in MTR method is determined according to the results obtained from the last k iterations. The residual norm ρ and solution norm η are calculated from Eq. (19)

and Eq. (20) respectively. The regularization parameter λ is determined by L-curve method. The regularized solution of the changes of the structural parameters is calculated from Eq. (18).

Step 7: The finite element model is updated.

Step 8: Repeat Steps 4 to 7 until the convergence condition in Eq. (8) is met.

5. Numerical examples

5.1 Simulation studies with a three-dimensional frame structure

A three-dimensional unsymmetrical frame structure shown in Fig. 2 is studied to illustrate the performance of the proposed method. The finite element model of the structure consists of 26 elements and 20 nodes each with six DOFs. The frame is fixed to the ground at Nodes 1 to 8 with rigid supports. The elastic modulus of material is 210 GPa, and the material density is 7.8×10^3 kg/m^3. The area of the member cross-section is 0.04 m^2. The flexural moment of inertias of all members in the x- and y-directions are 1.33×10^{-4} m^4. Rayleigh damping is assumed and the damping ratios for the first two modes are both taken as $\xi = 0.02$.

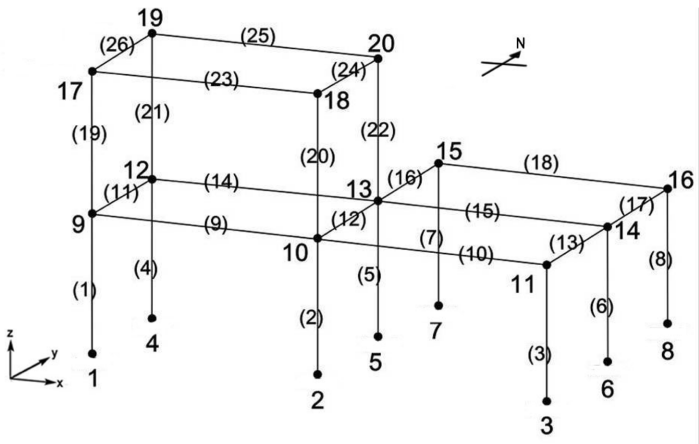

(a) Element no. and node no.
(•) denotes the element number

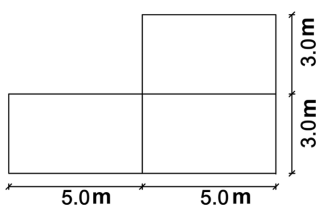

(b) Plan of the structure model

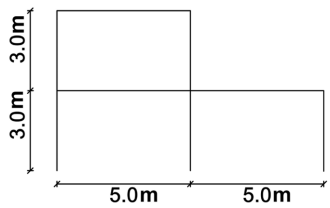

(c) Elevation of the structural model

Fig. 2 Finite element model of the three-dimensional frame structure

Table 1 Computation and iteration detail

Case no.	Method	Convergence error	Iteration no. required	Error (%) of identification
Case 1	TR	10^{-8}	35	7.65×10^{-4}
	MTR	10^{-8}	20	1.24×10^{-5}
Case 2	TR	10^{-4}	3	50.83
	MTR	10^{-4}	4	0.78
Case 3	TR	10^{-3}	6	52.19
	MTR	10^{-3}	6	1.24

The structure is subject to North-South El-Centro seismic acceleration acting along the *y*-axis of the supporting nodes. The equation of motion of the structural system becomes

$$\mathbf{M}\ddot{\mathbf{x}} + \mathbf{C}\dot{\mathbf{x}} + \mathbf{K}\mathbf{x} = -\mathbf{M}\Gamma\ddot{\mathbf{x}}_g \tag{28}$$

where Γ is a vector of zeros and ones defining the loading from ground acceleration onto the structure, $\ddot{\mathbf{x}}_g$ is the ground acceleration. The DOFs in *x*-direction at Nodes 10 and 15, *y*-direction at Nodes 10, 12, 13 and 14 and *z*-direction at Nodes 11 and 16 are taken as the sensor locations. The sampling rate and time are 500 Hz and 1s respectively.

The elastic modulus of material, E_i, is taken as the stiffness parameter to be identified in this study. The mass and damping of the system are assumed unchanged. The model errors that are simulated as random errors uniformly distributed within of the modulus of elasticity of material *E*.

The Tolerance in Eq. (8) is taken equal to 10^{-8}, 10^{-4} and 10^{-3} for different cases as listed in Table 1. The values $[l_{low}, l_{up}]$ in Eq. (16) are set equal to [−1.0, 0.1] and [−1.0, −0.02] for the studies with and without initial model errors respectively except otherwise stated.

5.2 Discussions on the identified results

A damage scenario with 15% reduction in the elastic modulus of elements 1 and 4 is studied with different levels of random noise and model errors.

To moderate the influence of noise, all the "measured" responses are fitted with the Chebyshev Polynomial. Take the acceleration response at *y*-direction of Node 14 as an example, the error versus number of terms of the Chebyshev Polynomial polluted with 10% noise is shown in Fig. 3 with the error defined as

$$error = \frac{\left\| Acc_{pollute} - Acc_{cf} \right\|_2}{\left\| Acc_{pollute} \right\|_2} \times 100\% \tag{29}$$

where $Acc_{pollute}$ denotes the "measured" acceleration matrix and Acc_{cf} denotes accelerations after curve fitting. The error is the smallest when the number of terms is 220, and the error remains relatively stable for a larger number of terms. Therefore, 220 terms are adopted in the Chebyshev Polynomial approximation of the acceleration response. Fig. 4 compares the polluted and curve-fitted responses at *y*-direction of Node 14. It can be seen that the Chebyshev Polynomial approximation is noted to be effective to remove the noise effect.

The TR and MTR methods are used to identify the damage scenarios described below.

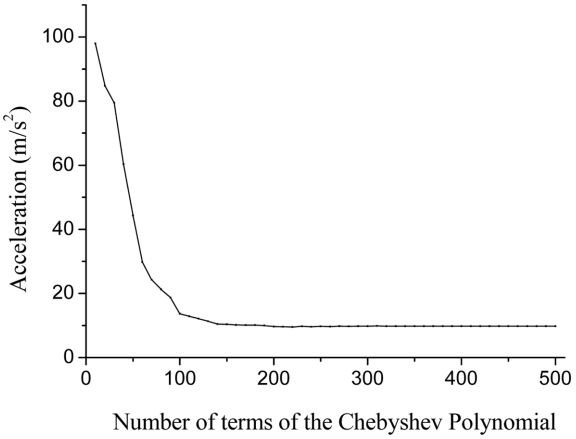

Fig. 3 Error versus number of terms of the Chebyshev Polynomial

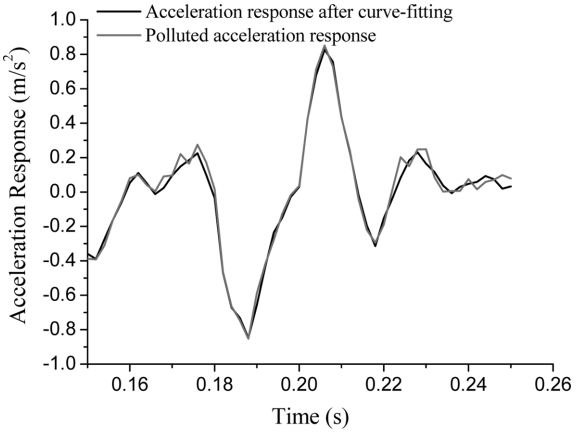

Fig. 4 Comparison of the polluted and curve-fitted responses at *y*-direction of Node 14

5.2.1 Case 1: without noise and model errors

Identified results from the TR method and the MTR method are plotted on the same graph for easy comparison. From Fig. 5 it can be found that the local damages are identified accurately with the two methods when there are no noise and model errors. Information on the computation requirements are given in Table 1. The evaluation of convergence error is computed from Eq. (8) and the error of identification is computed from Eq. (10). The convergence error for the two methods is 10^{-8}. The error computed from Eq. (8) for the TR method is $(7.65 \times 10^{-4})\%$ which is bigger than $(1.24 \times 10^{-5})\%$ for the MTR method.

5.2.2 Case 2: with 10% noise

When there is 10% noise in the measurements, results from the TR method are much poorer than those from the MTR method. The identification results from TR method diverge at the second step.

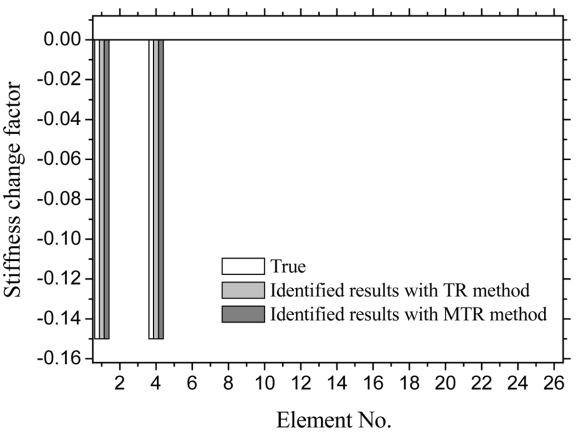

Fig. 5 Comparison of the identified results from the two methods for Case 1

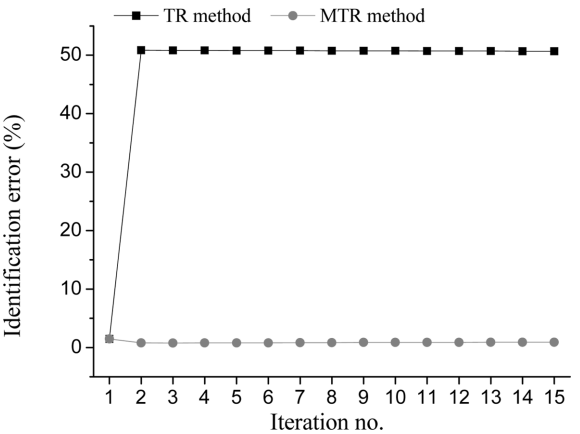

Fig. 6 Evolution of the error of identification with iterations for Case 2

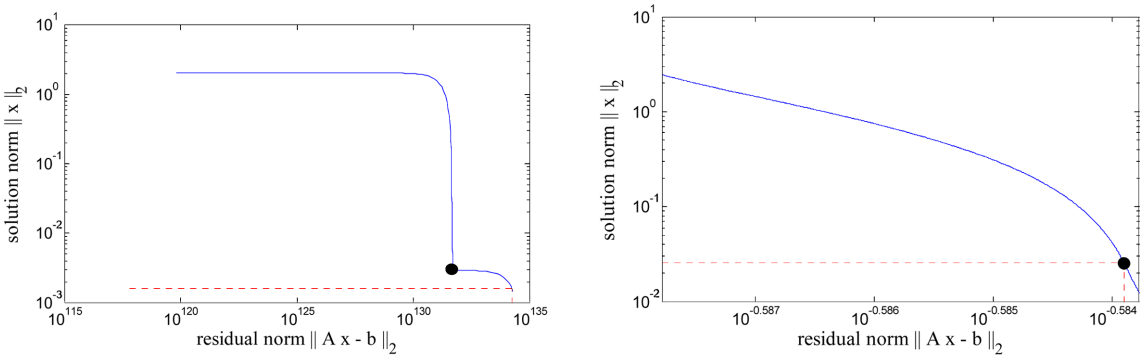

(a) L-curve of the third iteration from the TR method

(b) L-curve of the third iteration from the MTR method

Fig. 7 Comparison of L-curves and the regularization parameters from the two methods for Case 2

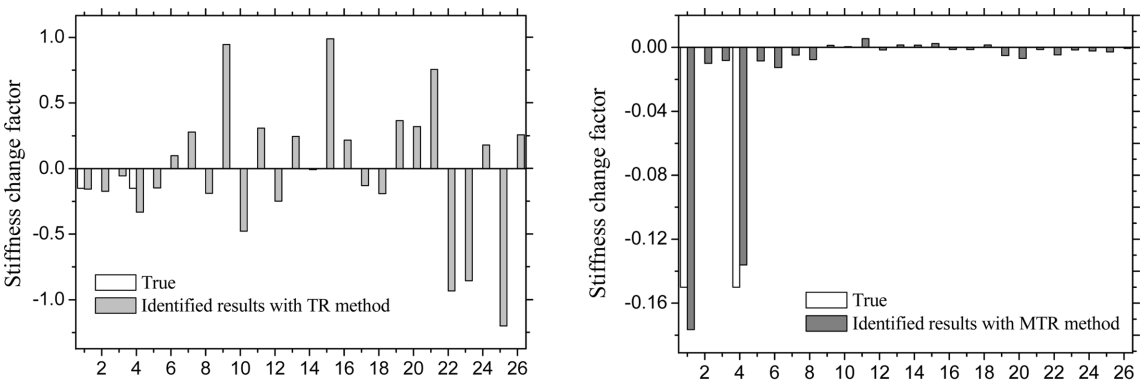

(a) TR method

(b) MTR method

Fig. 8 Comparison of the identified results from the two methods for Case 2

Here, diverge means that the regularization parameter dramatically changes and directs the regularization to a wrong path. Fig. 6 shows the evolution of the error of identification with iterations from the two methods. It is noted that the two methods are the same in the first iteration which is expected as they are based on the same initial condition. However, the identification results from TR method diverge at the second step and converge to a wrong path at the third step with a convergence error 10^{-4} while those from the MTR method converge to a steady value with the right path at the fourth step.

Figs. 7(a) and 7(b) show the L-curve and the regularization parameter with the two methods for the third and fourth iterations respectively. It is found that the regularization parameter for the TR method is extremely big with the value of 1.67×10^{138} and this parameter directs regularization to a wrong path. In MTR method, the regularization parameter is 0.33 and it only has a little change after the fourth iteration. It proves that the MTR method regularizes the solution in a consistent way.

Figs. 8(a) and 8(b) show the identified results with bar chart from the two methods. The errors computed from Eq. (8) are 50.83% and 0.67% for the TR and MTR methods respectively. It can be

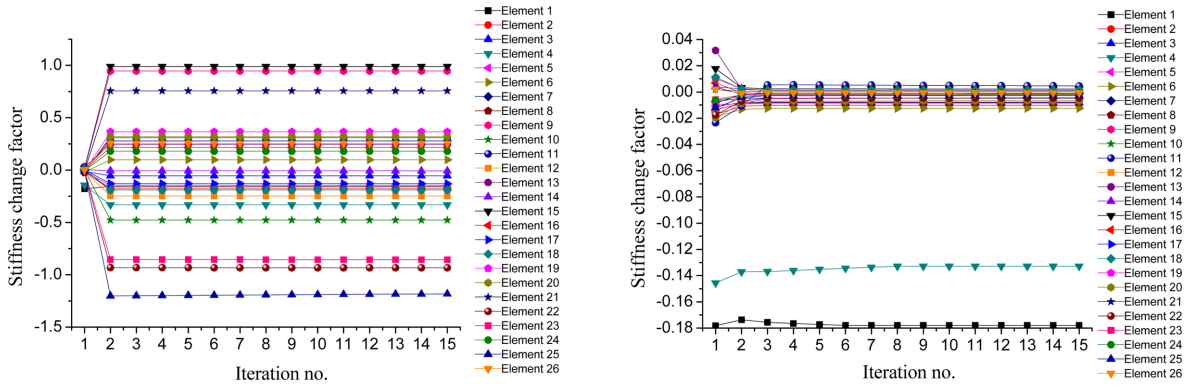

(a) TR method (b) MTR method

Fig. 9 Evolution of stiffness fractional change factor from the two method for Case 2

seen that almost all the elements are wrongly identified except the damaged element 1 in the TR method. The results obtained from the MTR method are noted to be much better than those obtained from the TR method with 10% noise in the measured responses. The location and extent of damages can be identified with acceptable errors from MTR method.

Figs. 9(a) and 9(b) show the evolution of the stiffness fractional change with iterations from the two methods. The identification results of the TR method are with larger errors in the identification results while those are with higher accuracy from the MTR method. The identified stiffness fractional changes converge to steady and relative accurate values after iterations.

5.2.3 Case 3: with 10% noise and 5% model errors

The followings give the comparative studies of the two methods for the case with 10% noise and 5% initial model errors that are simulated as random errors uniformly distributed within ±5% of the modulus of elasticity of material *E*. Fig. 10 shows the evolution of the error of identification with iterations from the two methods. The identification results from TR method diverge at the second

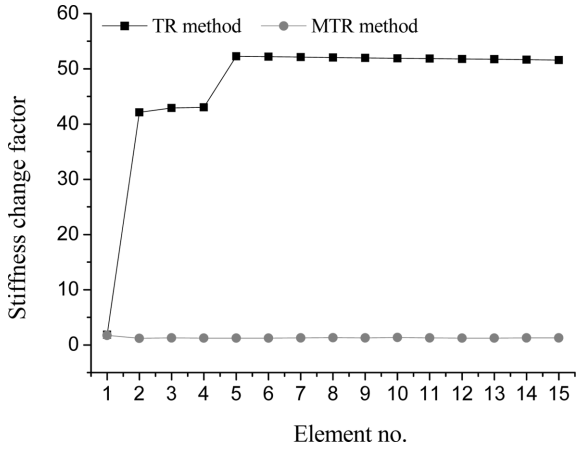

Fig. 10 Evolution of the error of identification with iterations for Case 3

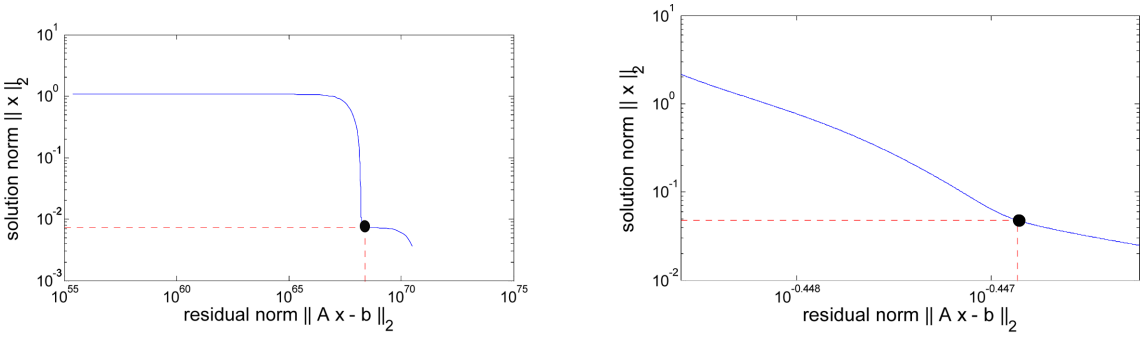

(a) L-curve of the third iteration from the TR method (b) L-curve of the third iteration from the MTR method

Fig. 11 Comparison of L-curves and the regularization parameters from the two methods for Case 3

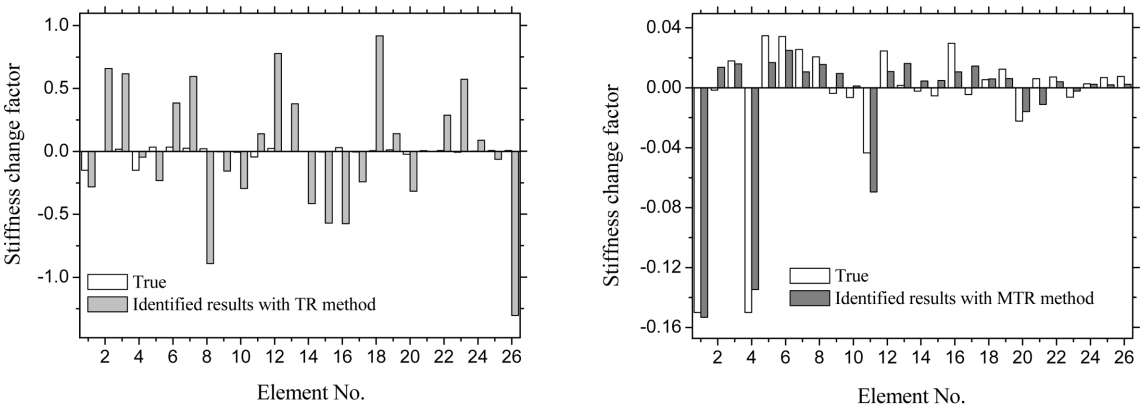

(a) TR method (b) MTR method

Fig. 12 Comparison of the identified results from the two methods for Case 3

step and converge to a wrong path at the sixth step with a convergence error 10^{-3} while those from the MTR method converge to a steady value with the right path at the sixth step.

Figs. 11(a) and 11(b) show the L-curve and the regularization parameter with the two methods for the sixth iteration respectively. Similar to Case 1, the regularization parameter for the TR method is extremely big with the value of 8.79×10^{70} and this parameter directs the regularization to a wrong path. In the MTR method, the regularization parameter is 0.28 and it has a little change after the sixth iteration.

The errors computed from Eq. (8) are 52.19% and 1.24% for the TR and MTR methods respectively. Fig. 12(a) and 12(b) show the identified results with bar chart from the two methods. In the TR method the physical meaning of the solution is not ensured, and the errors of the identified results are too big to be acceptable. The errors of identification results from the MTR method which has limits on the identified results are slightly small. There are only few wrongly identified elements with small model errors and the stiffness parameters of other elements can be identified accurately.

Figs. 13(a) and 13(b) show the evolution of the stiffness fractional change with iterations from the

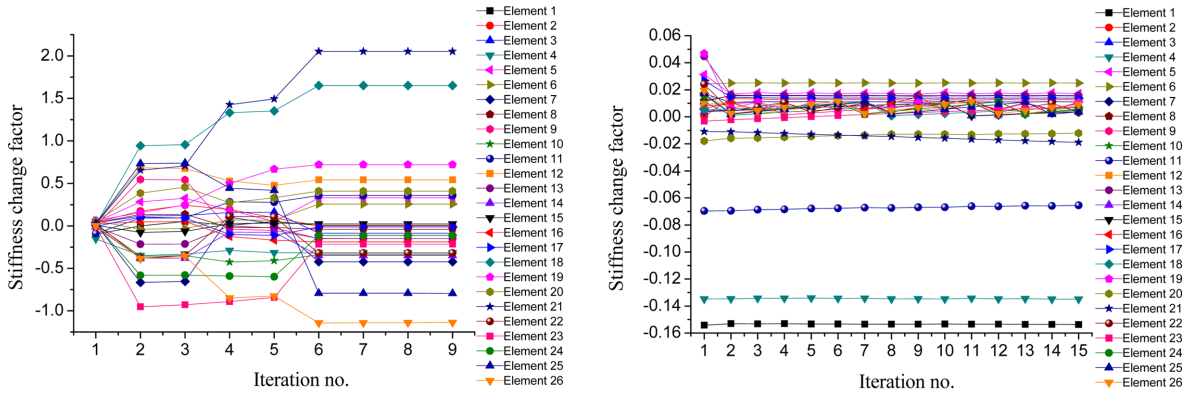

(a) TR method (b) MTR method

Fig. 13 Evolution of stiffness fractional change factor from the two method for Case 3

Table 2 Computation and iteration detail (Scenarios with different limits)

Scenario	Limits of the identified parameter	Convergence error	Iteration no. required	Regularization Parameter	Error (%) of identification
1	[−1, 0.1]	10^{-3}	6	0.28	1.24
2	[−1, 0.15]	10^{-3}	3	0.31	1.43
3	[−1, 0.2]	10^{-3}	6	0.32	1.30

two methods. The TR method has larger identification errors in almost all the elements. The identification results are with higher accuracy from the MTR method and the identified stiffness fractional changes converge to steady and relative accurate values after iterations.

5.2.4 The influence of limits

To investigate the influence of limits of l_{up} and l_{low} on the identification accuracy in MTR method, the limits of [−1, 0.1], [−1, 0.15], [−1, 0.2] are applied in the reference term in Eq. (16). The computation results are listed in Table 2. It is found that the identification error with the limit range [−1, 0.1] is the smallest and the errors with the other two limit ranges are very close to that with limit range [−1, 0.1]. It can be concluded that a proper limit range is [−1, l_{up}], in which l_{up} should be smaller than 1. The error of identification result will be small if l_{up} is set close to the upper range of the real model errors.

6. Conclusions

A Modified Tikhonov Regularization Method for model updating is presented in this paper for the case where there are both measurement noise and model errors in the structural system. The conventional Tikhonov Regularization Method has been shown to diverge after a few iterations in the computation. The proposed Regularization Method imposes limits on the fractional change of the physical parameters in the determination of the regularization parameter to allow for the

presence of initial model errors which may be above or below the analytical value. A side condition changes adaptively according to the results obtained in previous iterative steps to ensure the solution is in a realistic range. Chebyshev polynomial is applied to approximate the acceleration responses for moderating the influence of measurement noise. A three-dimensional unsymmetrical frame structure with different damage scenarios is studied to illustrate the proposed method. Results from simulations show that the proposed method has superior performance than the conventional TR method when there are both measurement noise and model errors.

Acknowledgements

The work described in this paper was supported by a research grant from National Science Foundation for Distinguished Young Scholars of China (Grant No. 50725826). The authors would also like to thank the funding supported from National Science Foundation of China (Grant No. 90815021). The authors are very thankful to Prof. S. S. Law and Dr X. Y. Li of The Hong Kong Polytechnic University for their valuable advices.

References

Bicanic, N. and Chen, H.P. (1997), "Damage identification in framed structures using natural frequencies", *Int. J. Num. Meth. Eng.*, **40**(23), 4451-4468.

Cawley, P. and Adams, R.D. (1979), "The location of defects in structures from measurements of natural frequencies", *J. Strain. Anal. Eng. Deg.*, **14**(2), 49-57.

Golub, G.H. and Van Loan, C.F. (1996), *Matrix Computations*, Johns Hopkins University Press, Baltimore, MD.

Hansen, P.C. (1987), "The truncated SVD as a method for regularization", *Bit. Num. Math.*, **27**(4), 534-553.

Hansen, P.C. (1992), "Analysis of discrete ill-posed problems by means of the L-curve", *Soc. Ind. appl. Math.*, **34**(4), 561-580.

Hassiotis, S. and Jeong, G.D. (1993), "Assessment of structural damage from natural frequency measurements", *Comput. Struct.*, **49**(4), 679-691.

Li, X.Y. and Law, S.S. (2010), "Adaptive Tikhonov regularization for damage detection based on nonlinear model updating", *Mech. Syst. Signal. Pr.*, **24**(6), 1646-1664.

Lu, Z.R. and Law, S.S. (2007), "Features of dynamic response sensitivity and its application in damage detection", *J. Sound. Vib.*, **303**(1-2), 305-329.

Ni, H.D. and Chen, Y. (2009), "The research of Chebyshev Polynomials' Fitting applied in vehicle navigation", *GNSS. World. China*., **6**, 37-42.

Osegueda, R.A., Carrasco, C.J. and Meza, R. (1997), "A modal strain energy distribution method to localize and quantify damage", *Proceedings of the 15th International Modal Analysis Conference*, Orlando, Florida, February.

Pandey, A.K., Biswas, M. and Samman, M.M. (1991), "Damage detection from changes in curvature mode shapes", *J. Sound. Vib.*, **145**(2), 321-332.

Tikhonov, A.N. (1963), "Solution of incorrectly formulated problems and the regularization method", *Soviet. Math. Dokl.*, **4**, 1035-1038.

Titurus, B. and Friswell, M.I. (2008), "Regularization in model updating", *Int. J. Numer. Meth. Eng.*, **75**(4), 440-478.

Toksoy, T. and Aktan, A.E. (1994), "Bridge-condition assessment by modal flexibility", *Exp. Mech.*, **34**(3), 271-278.

Vogel, C.R. (2002), *Computational Methods for Inverse Problems*, Frontiers in Applied Mathematics, SIAM, Philadelphia, PA.

Weber, B., Paultre, P. and Proulx, J. (2009), "Consistent regularization of nonlinear model updating for damage identification", *Mech. Syst. Signal. Pr.*, **23**(6), 1965-1985.